

Absorption Spectroscopy of Singlet CH<sub>2</sub> near 9500 cm<sup>-1</sup>†

Kaori Kobayashi,‡ Leah D. Pride,§ and Trevor J. Sears\*

Department of Chemistry, Brookhaven National Laboratory, Upton, New York 11973-5000

Received: January 24, 2000; In Final Form: March 22, 2000

The  $\tilde{b}^1B_1-\tilde{a}^1A_1$  spectrum of methylene between 9317 and 9610 cm<sup>-1</sup> was recorded using frequency-modulated diode laser absorption spectroscopy. This is the lowest-energy region ever observed in the CH<sub>2</sub>( $\tilde{b}^1B_1$ ) electronic state. Transitions to four upper rovibronic levels were identified using known ground-state combination differences. On the basis of comparison with published results of ab initio calculations, they were assigned to levels with both  $\tilde{a}$  and  $\tilde{b}$  primary electronic wave function character:  $K = 0 \tilde{b} (0,1,0)$ ,  $K = 4 \tilde{b} (0,0,0)$ ,  $K = 1 \tilde{a} (0,8,0)$ , and  $K = 0 \tilde{b} (0,2,0)$ . The first three of these levels had not previously been observed. The rotational assignments of the last,  $K = 0 \tilde{b} (0,2,0)$ , observed via transitions from the  $\tilde{a} (0,1,0)$  vibrationally hot bending level, differ from the original assignments of Herzberg and Johns [*Proc. R. Soc. London, Ser. A* **1966**, 295, 107]. A comparison with the results of the most recent high-level quantum chemical calculations suggests that further refinement of the potential energy surface of the  $\tilde{b}$  state near its equilibrium would be desirable.

## Introduction

Methylene is a fundamental radical intermediate species whose study has driven the development of theoretical and experimental techniques. It has two outer electrons to be distributed between  $a_1$  and  $b_1$  symmetry orbitals, and the change of spin configuration within them gives rise to a triplet ground state,  $\tilde{X}^3B_1$ , and singlet low-lying states,  $\tilde{a}^1A_1$  and  $\tilde{b}^1B_1$ . The singlet–triplet splitting ( $\Delta E_{ST}$ ) strongly influences the radical's chemical behavior. It was first definitively measured using laser magnetic resonance (LMR) to detect mutually perturbing singlet- and triplet-state levels.<sup>1</sup> Subsequent analysis<sup>2</sup> showed that the  $\tilde{a}$  state lies above the ground state by only 3147 ± 5 cm<sup>-1</sup>. The two singlet levels correlate with a degenerate  $^1\Delta_g$  state at linearity, but coupling between the electronic orbital angular momentum ( $\Lambda$ ) and the bending vibrational angular momentum ( $I$ ), known as the Renner-Teller effect,<sup>3</sup> splits the electronic (and vibrational) degeneracy. In CH<sub>2</sub>, this results in a lowering of the electronic energy as the molecule bends and two distinct, nondegenerate, surfaces. The bending vibronic levels are now conventionally labeled by the quantum number  $K$  ( $K = \Lambda + I$ ) where  $K$  represents  $K_a$ , the projection of the total angular momentum,  $J$ , on the  $a$  inertial axis. The wave functions of levels with  $K \neq 0$  contain mixtures of the unperturbed electronic functions. This effect is normally illustrated by plots of the variation in the potential energy surfaces as a function of the bending angle, such as shown for CH<sub>2</sub> in Figure 1. The energy of the linear configuration, that is, the barrier to the linearity in the two states, is a quantity that has still to be measured accurately, although many calculations have focused on this and other properties of the bending potential surfaces [see below].

Transitions between these singlet states fall into the near-infrared to visible region. Herzberg<sup>4</sup> first reported the spectrum

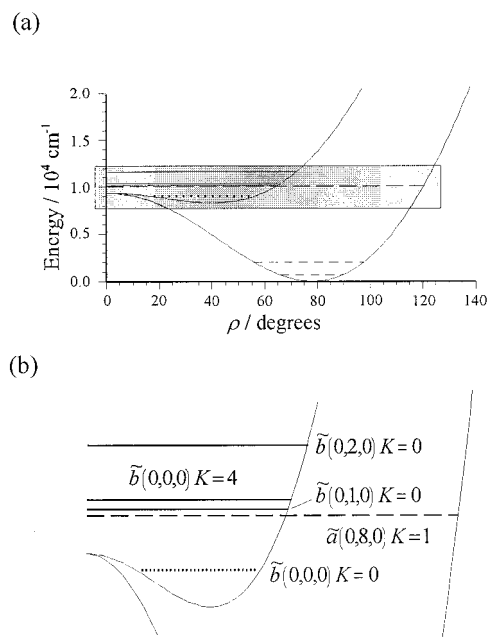


**Figure 1.** (a) A cut through the potential energy surfaces for the  $\tilde{a}$  and  $\tilde{b}$  states of CH<sub>2</sub> along the bending angle coordinate, computed from the results of Duxbury and Jungen.<sup>8</sup> (b) Boxed section of (a) expanded to show the selected  $\tilde{b}$  levels clearly.

of singlet methylene in the visible region and subsequently, Herzberg and Johns analyzed it in detail.<sup>5</sup> The Renner-Teller effect and spin–orbit coupling between the ground triplet state and the singlet states, as well as local anharmonic and Coriolis interactions involving all three states, severely perturb both the  $\tilde{a}$  and  $\tilde{b}$  state rovibrational energy levels; these energy levels therefore exhibit very irregular spacings, making spectral analysis difficult. Spectroscopic analyses have generally relied upon ground-state combination differences to confirm energy level positions. Recent experimental work has also been guided by ab initio molecular orbital calculations of increasing accuracy. A similar situation is encountered in NH<sub>2</sub>.<sup>6</sup> In view of the

† Part of the special issue "C. Bradley Moore Festschrift".

\* To whom correspondence should be addressed at Brookhaven National Laboratory.

‡ Brookhaven National Laboratory.

§ ERULF Student at the Department of Chemistry, Brookhaven National Laboratory. Present address: Department of Chemical Technology, New York City Technical College, Brooklyn, New York 11201.

experimental difficulties and its prototypical nature, methylene has been a favorite benchmark for high-level quantum calculations. Green et al.<sup>7</sup> calculated ab initio potential energy surfaces (PESs) and also obtained rovibronic energy levels by solving the vibrational problem using the calculated surfaces. The separation of the singlet potential energy surfaces was empirically adjusted from their calculated value to reproduce several observed  $\tilde{b}$ – $\tilde{a}$  transitions. Duxbury et al.<sup>8–11</sup> have also carried out a series of studies on the singlet–singlet transition, and their spectroscopic analyses have identified many specific perturbations among the vibronic levels. Finally, the ab initio potential of Green et al.<sup>7</sup> was modified more substantially by Gu et al.,<sup>12</sup> who fit rovibronic energies derived from the experimental  $\tilde{b}$ – $\tilde{a}$  spectral data available to them at the time to the Morse oscillator rigid-bender internal dynamics (MORBID) model modified to include the Renner effect.<sup>13,14</sup> At the time, the available spectroscopic data did not contain information on the region close to the equilibrium energy of the  $\tilde{b}$  state; hence, assessing the reliability of the surfaces in this region is difficult. All recent calculations conclude that, in the  $\tilde{b}$  state, only the lowest few rotational levels in the (0,0,0) level at about 8350  $\text{cm}^{-1}$  above the zero-point level of the  $\tilde{a}$  state are located below the barrier to linearity where the  $\tilde{a}$  and  $\tilde{b}$  states become degenerate.

Following Herzberg and Johns,<sup>4,5</sup> many experimental studies have been carried out using laser-based techniques. The earliest laser studies employed modest resolution, by modern standards. These studies added little spectroscopic information to that known from the classical work but focused on measuring the singlet–triplet splitting.<sup>15,16</sup> More recently, the visible region was surveyed at high resolution, and about 10 000 absorption lines were observed.<sup>17,18</sup> However, only about 5% of the spectral lines were assigned because of the complexity and irregularity of the observed spectrum and an incomplete knowledge of the low-lying energy levels of singlet methylene. The  $\tilde{a}$  (0,0,0) and the  $\tilde{a}$  (0,1,0) levels were, however, characterized, and some specific perturbations caused by spin–orbit coupling with vibrationally excited triplet state levels were identified. Splittings in several rotational levels<sup>17</sup> and anomalous Zeeman effects are the direct results of this interaction. Stretching vibration–rotation spectra of the  $\tilde{a}$  state were also recorded and analyzed, including Coriolis coupling between the symmetric and antisymmetric vibrations.<sup>19,20</sup> Using the fitted molecular constants, the equilibrium structure of the  $\tilde{a}$  state was estimated. Vibrationally excited levels of the  $\tilde{a}$  state as high as 6757  $\text{cm}^{-1}$  have been observed by laser-induced fluorescence (LIF),<sup>21</sup> stimulated emission pumping,<sup>22,23,24</sup> and dispersed fluorescence.<sup>25–27</sup> LIF<sup>28</sup> and dispersed fluorescence<sup>29</sup> were also utilized to further characterize the visible  $\tilde{b}$ – $\tilde{a}$  spectrum. Transitions in the same band system in the near-infrared region have smaller Franck–Condon factors, and the absorption spectra in this region were only observed rather recently.<sup>30–32</sup> A frequency-modulated absorption spectrometer that realizes higher sensitivity was used in the latter two studies,<sup>31,32</sup> and spectra as low as 9787  $\text{cm}^{-1}$  were recorded. A very recent review of frequency modulation spectroscopy of transient molecules provides a good introduction to the technique.<sup>29</sup>

In this study, we began a search for the  $K = 0$   $\tilde{b}$  (0,1,0) level and  $K = 4$   $\tilde{b}$  (0,0,0) levels, predicted to lie at energies of 9537 and 9754  $\text{cm}^{-1}$ , respectively, above the zero-point level of the  $\tilde{a}$   $^1A_1$  state.<sup>12</sup> This region of the  $\tilde{b}$ – $\tilde{a}$  spectrum remained unexplored, and while it is still above the barrier to linearity, it lies substantially below others so far detected. Despite the experimental disadvantage of generally smaller Franck–Condon factors compared with the shorter wavelength region, the

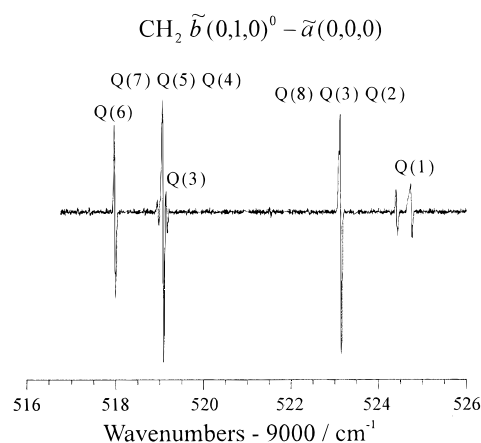


**Figure 2.** The  $Q$ -branch structure of  $K = 0$   $\tilde{b}$  (0,1,0) of  $\text{CH}_2$  near 9520  $\text{cm}^{-1}$ . Several transitions are overlapped in this region.

information contained in such spectra on the shape of the PES near the barrier is very important because the energy levels in this region are very sensitive to details of the PES. In addition, less dense spectral structure is expected in this region, because the vibronic level density is lower, and the analysis will aid future assignments in the higher frequency region where spectra are more congested.

## Experiment

The details of the spectrometer are described elsewhere.<sup>32</sup> The major difference lies in the use of a different high-speed photoreceiver (New Focus, model 1611) incorporating an InGaAs PIN photodiode because the Si-based detector used previously has poor response at the longer wavelengths used here. The diode laser was an Environmental Optical Sensors model 2010, in which the laser cavity has better mechanical stability compared to that used previously. Methylene was generated by 308-nm laser photolysis of ketene, which is known to be an efficient reaction for producing methylene in  $\tilde{a}$  (0,0,0) and  $\tilde{a}$  (0,1,0) levels. The total pressure of ketene and He (in large excess) was maintained at about 2.3 Torr during the experiment. A multipass Herriott-type cell<sup>34,35</sup> was used to maximize the overlap of the photolysis laser and probing diode laser beams and to extend the absorption length. In the Herriott configuration, two identical spherical mirrors are separated by slightly less than their radius of curvature, and the probe laser beams traverse off-axis paths between them. In our configuration, the photolysis laser beam is aligned along the central axis of the cell between one-inch diameter holes cut in the centers of the end mirrors. The probe laser beam is reflected from a series of points around the annular mirror surface. Three circuits of the mirrors with six spots on each mirror circuit resulting in 35 passes through the 1.1-m cell were used in most of the measurements. The averaged data of 30 excimer laser shots was collected at each point. About 400 lines were observed from 9317 to 9610  $\text{cm}^{-1}$ . This number shows the less dense structure of spectra here, compared with 1288 lines between 10021.9 and 10605.5  $\text{cm}^{-1}$  observed previously.<sup>32</sup> Repeated measurements over a short region of the spectrum gave a reproducibility of 0.003  $\text{cm}^{-1}$  in the measured line positions; however, combination differences obtained from several widely spaced transitions for a number of levels suggest an accuracy of 0.02  $\text{cm}^{-1}$  over the entire region. As an example of the recorded spectra, the  $Q$ -branch region of the  $K = 0$   $\tilde{b}$  (0,1,0)– $\tilde{a}$  (0,0,0) band is shown in Figure 2.

TABLE 1: Observed Transitions in the near Infrared Spectrum of  $\tilde{a} \ ^1A_1$  CH<sub>2</sub>

$J'_{KaKc}$	$J''_{KaKc}$	$\nu^a$	(intensity)	$J'_{KaKc}$	$J''_{KaKc}$	$\nu^a$	(intensity)
$\tilde{b} (0,1,0)^0 - \tilde{a} (0,0,0)$				$\tilde{b} (0,2,0)^0 - \tilde{a} (0,1,0)$			
0 <sub>00</sub>	1 <sub>10</sub>	9505.247	(0.0113)	0 <sub>00</sub>	1 <sub>10</sub>	9441.192	(0.0027)
1 <sub>01</sub>	1 <sub>11</sub>	9524.745	(0.0083)	1 <sub>01</sub>	1 <sub>11</sub>	9460.983	(0.0049)
1 <sub>01</sub>	2 <sub>11</sub>	9479.974	(0.0071)	1 <sub>01</sub>	2 <sub>11</sub>	9415.735	(0.0071)
2 <sub>02</sub>	1 <sub>10</sub>	9551.406	(0.0025)	2 <sub>02</sub>	1 <sub>10</sub>	9487.450	(0.0095)
2 <sub>02</sub>	2 <sub>12</sub>	9523.124	(0.0857) <sup>b</sup>	2 <sub>02</sub>	2 <sub>12</sub>	9459.669	(0.0183)
2 <sub>02</sub>	3 <sub>12</sub>	9450.714	(0.0148)	2 <sub>02</sub>	3 <sub>12</sub>	9386.187	(0.0128)
3 <sub>03</sub>	2 <sub>11</sub>	9554.732	(0.0007)	3 <sub>03</sub>	2 <sub>11</sub>	9492.828	(0.0066)
3 <sub>03</sub>	3 <sub>13</sub>	9519.161	(0.0088)	3 <sub>03</sub>	3 <sub>13</sub>	9458.346	(0.0078)
3 <sub>03</sub>	4 <sub>13</sub>	9416.541	(0.0047)	3 <sub>03</sub>	3 <sub>31</sub>	9343.839	(0.0008)
3 <sub>03</sub>	2 <sub>11</sub>	9558.696	(0.0013)	3 <sub>03</sub>	4 <sub>13</sub>	9353.246	(0.0099)
3 <sub>03</sub>	3 <sub>13</sub>	9523.124	(0.0857) <sup>b</sup>	4 <sub>04</sub>	3 <sub>12</sub>	9493.788	(0.0200)
3 <sub>03</sub>	4 <sub>13</sub>	9420.509	(0.0030)	4 <sub>04</sub>	3 <sub>30</sub>	9405.054 <sup>d</sup>	(0.0004)
4 <sub>04</sub>	3 <sub>12</sub>	9557.542	(0.0075)	4 <sub>04</sub>	4 <sub>14</sub>	9457.262	(0.0234)
4 <sub>04</sub>	4 <sub>14</sub>	9519.076	(0.0636) <sup>b</sup>	4 <sub>04</sub>	5 <sub>14</sub>	9319.624	(0.0118)
4 <sub>04</sub>	4 <sub>32</sub>	9406.069	(0.0005) <sup>b</sup>	5 <sub>05</sub>	4 <sub>13</sub>	9491.763	(0.0087)
4 <sub>04</sub>	5 <sub>14</sub>	9385.101	(0.0130)	5 <sub>05</sub>	5 <sub>15</sub>	9458.006	(0.0060)
5 <sub>05</sub>	4 <sub>13</sub>	9556.877	(0.0021)	6 <sub>06</sub>	5 <sub>14</sub>	9489.124	(0.0168)
5 <sub>05</sub>	5 <sub>15</sub>	9519.076	(0.0636) <sup>b</sup>	6 <sub>06</sub>	5 <sub>32</sub>	9401.992 <sup>d</sup>	(0.0016)
5 <sub>05</sub>	6 <sub>15</sub>	9354.079	(0.0021)	6 <sub>06</sub>	6 <sub>16</sub>	9458.513	(0.0337)
6 <sub>06</sub>	5 <sub>14</sub>	9553.297	(0.0057) <sup>c</sup>	7 <sub>07</sub>	6 <sub>15</sub>	9487.073	(0.0087)
6 <sub>06</sub>	5 <sub>32</sub>	9476.042	(0.0043) <sup>d</sup>	7 <sub>07</sub>	7 <sub>17</sub>	9461.295	(0.0062)
6 <sub>06</sub>	6 <sub>16</sub>	9517.992	(0.0316)	8 <sub>08</sub>	7 <sub>16</sub>	9487.169	(0.0191)
6 <sub>06</sub>	6 <sub>34</sub>	9369.580	(0.0009)	8 <sub>08</sub>	8 <sub>18</sub>	9465.648	(0.0115)
6 <sub>06</sub>	7 <sub>16</sub>	9318.733	(0.0049)				
6 <sub>06</sub>	7 <sub>16</sub>	9325.156	(0.0052)				
7 <sub>07</sub>	6 <sub>15</sub>	9551.848	(0.0018)				
7 <sub>07</sub>	7 <sub>17</sub>	9519.076	(0.0636) <sup>b</sup>				
8 <sub>08</sub>	7 <sub>16</sub>	9548.151	(0.0008) <sup>c</sup>				
8 <sub>08</sub>	7 <sub>16</sub>	9554.564	(0.0019)				
8 <sub>08</sub>	8 <sub>18</sub>	9518.965	(0.0044)				
8 <sub>08</sub>	8 <sub>18</sub>	9523.124	(0.0857) <sup>b</sup>				
$\tilde{b} (0,0,0)^4 - \tilde{a} (0,0,0)$				$\tilde{a} (0,8,0)^1 - \tilde{a} (0,0,0)$			
4 <sub>40</sub>	3 <sub>30</sub>	9501.732	(0.0225)	1 <sub>10</sub>	0 <sub>00</sub>	9442.402	(0.0035)
4 <sub>40</sub>	4 <sub>32</sub>	9427.030 <sup>e</sup>		1 <sub>10</sub>	2 <sub>20</sub>	9342.769	(0.0003)
4 <sub>40</sub>	5 <sub>14</sub>	9406.069	(0.0005)	1 <sub>11</sub>	1 <sub>01</sub>	9427.524	(0.0017)
4 <sub>41</sub>	3 <sub>31</sub>	9501.980	(0.0104)	1 <sub>11</sub>	2 <sub>21</sub>	9347.261	(0.0009)
4 <sub>41</sub>	4 <sub>31</sub>	9426.160	(0.0010)	2 <sub>11</sub>	1 <sub>01</sub>	9455.901	(0.0048)
4 <sub>41</sub>	4 <sub>31</sub>	9423.410	(0.0016)	2 <sub>11</sub>	2 <sub>21</sub>	9375.653	(0.0006) <sup>b</sup>
5 <sub>41</sub>	4 <sub>31</sub>	9504.863	(0.0098)	2 <sub>11</sub>	3 <sub>03</sub>	9369.843	(0.0006)
5 <sub>41</sub>	5 <sub>33</sub>	9412.462	(0.0029)	2 <sub>12</sub>	2 <sub>02</sub>	9429.776	(0.0016)
5 <sub>42</sub>	4 <sub>32</sub>	9505.860	(0.0261)	2 <sub>12</sub>	3 <sub>22</sub>	9330.058	(0.0013)
5 <sub>42</sub>	5 <sub>32</sub>	9407.646	(0.0063)	3 <sub>12</sub>	2 <sub>02</sub>	9466.702	(0.0018)
5 <sub>42</sub>	5 <sub>14</sub>	9484.901	(0.0035) <sup>d</sup>	3 <sub>12</sub>	3 <sub>22</sub>	9366.981	(0.0003) <sup>c</sup>
6 <sub>42</sub>	5 <sub>32</sub>	9501.510	(0.0093)	3 <sub>12</sub>	4 <sub>04</sub>	9351.357	(0.0003)
6 <sub>42</sub>	5 <sub>50</sub>	9340.645	(0.0007)	3 <sub>13</sub>	3 <sub>03</sub>	9436.309	(0.0028)
6 <sub>42</sub>	6 <sub>34</sub>	9395.053	(0.0026)	3 <sub>13</sub>	3 <sub>24</sub>	9382.114	(0.0008)
6 <sub>42</sub>	5 <sub>14</sub>	9578.765	(0.0036) <sup>d</sup>	4 <sub>13</sub>	3 <sub>03</sub>	9476.915	(0.0060)
6 <sub>42</sub>	6 <sub>16</sub>	9543.517	(0.0010)	4 <sub>13</sub>	3 <sub>21</sub>	9422.715	(0.0017)
6 <sub>42</sub>	7 <sub>16</sub>	9350.654	(0.0007)	4 <sub>13</sub>	4 <sub>23</sub>	9355.837	(0.0042)
				4 <sub>13</sub>	5 <sub>05</sub>	9333.876	(0.0006)
				4 <sub>14</sub>	3 <sub>22</sub>	9426.119	(0.0003)
				4 <sub>14</sub>	4 <sub>04</sub>	9445.486	(0.0028)
				4 <sub>14</sub>	4 <sub>22</sub>	9375.689	(0.0009) <sup>b</sup>

<sup>a</sup> In wavenumbers (cm<sup>-1</sup>). Estimated measurement accuracy is  $\pm 0.003$  cm<sup>-1</sup> for closely spaced lines,  $\pm 0.02$  cm<sup>-1</sup> over the entire region. <sup>b</sup> Overlapped line. <sup>c</sup> Laser noisy, poorer measurement accuracy than usual. <sup>d</sup> Line apparently anomalously strong or weak. <sup>e</sup> Estimated position from partial data because of mode break.

## Analysis

Four rovibronic levels,  $K = 0 \tilde{b} (0,1,0)$ ,  $K = 0 \tilde{b} (0,2,0)$ ,  $K = 4 \tilde{b} (0,0,0)$ , and  $K = 1 \tilde{a} (0,8,0)$ , were assigned, based on the known rotational combination differences of the  $\tilde{a} (0,0,0)$  or  $\tilde{a} (0,1,0)$  levels.<sup>17</sup> While the combination differences identify the upper-state  $K$  values, we were guided by Gu et al.'s calculation<sup>12</sup> as to vibronic assignments because their results showed fair to good agreement with experimental values in previous studies.<sup>32</sup> Ninety-two assigned transitions, including some obeying  $\Delta K = \pm 3$  selection rules, are listed in Table 1. The energy levels of the upper states, determined from the spectra and known

lower-level energies, all lie above the estimated barrier to linearity and were fit to a pseudolinear molecule rotational Hamiltonian by using the effective term value and rotational, centrifugal distortion and  $l$ -type splitting constants:

$$F(J,K) = \nu_0 + B_v J(J+1) - D_v J^2(J+1)^2 \pm \frac{q_v}{2} J^K(J+1)^K \quad (1)$$

Here,  $\nu_0$ ,  $B_v$ ,  $D_v$ , and  $q_v$  denote hypothetical rotationless term values, the effective rotational, centrifugal, and  $l$ -type doubling constants for the vibrational level  $\nu$ . Note the relationship

**TABLE 2: Molecular Constants for Assigned Upper Levels (in  $\text{cm}^{-1}$ )<sup>a</sup>**

level	$K$	$\nu_0$	$B_v$	$D_v$	$q_v$
$\tilde{b}(0,1,0)$	0	9536.52(91)	7.69(12)	0.0010(28)	-
$\tilde{b}(0,2,0)$	0	10 827.022(67)	7.6990(90)	0.00002(23)	-
$\tilde{b}(0,0,0)$	4	9551.98(21)	7.961(16)	0.00169(29)	-0.000000105(40)
$\tilde{a}(0,8,0)$	1	9426.51(31)	8.796(72)	0.0114(31)	-1.661(18)

<sup>a</sup> One standard deviation is given in parentheses.

between  $K$  and  $l$  ( $K = l \pm \Lambda$ )<sup>3</sup> and also the bent and linear molecule limit bending vibrational quantum numbers used by various authors:<sup>7–13</sup>

$$\nu_2(\text{linear}) = 2\nu_2(\text{bent}) + |K \mp 2| \quad (2)$$

The minus sign applies for the  $\tilde{a}$  electronic state and the plus sign for the  $\tilde{b}$  state. In this work, the bent molecule notation is used. Also, we introduce the notation  $(0,1,0)^0$  and so forth for  $K = 0$ ,  $(0,1,0)$ . The results of the fits are summarized in Table 2. The differences between the observed and calculated energies are usually of the order of  $0.1\text{--}0.5 \text{ cm}^{-1}$ , which is much larger than the experimental errors. Only  $\tilde{b}(0,0,0)^4$  was well modeled in this way. However, we did find the fits useful for predicting the approximate positions of additional transitions in a band during the spectral assignments.

Other vibronic levels may be spectroscopically accessible in this region. For example, according to the Gu et al. results,<sup>12</sup> the  $\tilde{b}(0,1,0)^3\text{--}\tilde{a}(0,1,0)$  transition has reasonable intensity, and some rotational transitions would lie in the region covered here. Note that in ref 12, two energies are attributed to the same  $\tilde{b}(0,1,0)^3$  level. Marr et al.<sup>32</sup> assigned one of them following detection of the  $\tilde{b}(0,1,0)^3\text{--}\tilde{a}(0,0,0)$  transition near  $10500 \text{ cm}^{-1}$ . Comparison with other computational results<sup>10,11</sup> suggests that the other seems actually to correspond to  $\tilde{a}(0,9,0)^3$ . We could not make convincing assignments to a second  $K = 3$  level in the present data. In fact, only two transitions are predicted to lie in the spectral region covered, but the observation still suggests that this transition is not as strong as expected. Actually, the simple Franck–Condon factors of Green et al.’s results<sup>7</sup> indicate about a 5-times weaker intensity for this transition compared with  $\tilde{b}(0,1,0)^3\text{--}\tilde{a}(0,0,0)$  observed by Marr et al. This is certainly reasonable if we consider the level to possess considerable  $\tilde{a}(0,9,0)^3$  character.

## Discussion

For the levels originally targeted in this investigation, we have detected 31 transitions to the  $\tilde{b}(0,1,0)^0$  level, and the upper-level positions are confirmed by the observation of all the expected rovibronic transitions that match the known ground-state combination differences. In addition, a local rotational perturbation was observed in this level. The  $3_{03}$  level was split into two, and both sets of transitions showed relative intensities, in approximate agreement with the Hönl–London factors for a  $K = 0$  level.<sup>3</sup> The difference between the observed and the calculated rotational energy is shown in Figure 3. A source for this perturbation might lie in close proximity of the  $\tilde{a}(1,1,2)^2$  level.<sup>12</sup> Figure 4 illustrates the situation. If we accept this explanation, then similar shifts in the  $J = 2, 3$ , and possibly 4 levels would be suggested by Gu et al.’s calculation because the calculated energy levels of  $\tilde{a}(1,1,2)^2$  differ by only a few wavenumbers from those measured for  $\tilde{b}(0,1,0)^0$ . However, no other transitions to the perturbing level were identified in the data, implying that, in fact, the near resonance lies at the  $J = 3$  level only. The  $\tilde{b}(0,0,0)^4$  level is similarly well-determined, although fewer rotational transitions were observed to this

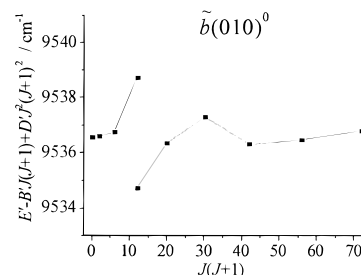


**Figure 3.** Rotational perturbation at  $J = 3$  in the  $\tilde{b}(0,1,0)^0$  level illustrated by the deviation of the measured energies at  $J = 3$  from the expected value calculated using the parameters in Table 2.

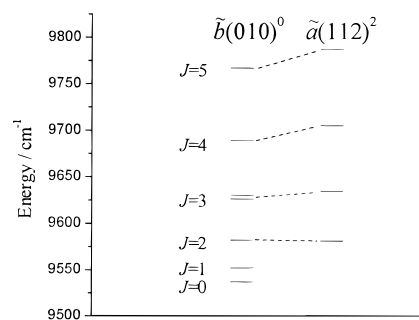


**Figure 4.** Rotational energy levels of  $K = 0 \tilde{b}(0,1,0)$  and  $K = 2 \tilde{a}(1,1,2)^2$ . The  $\tilde{b}(0,1,0)^0$  levels are observed, whereas the  $\tilde{a}(1,1,2)^2$  level positions are calculated by Gu et al.<sup>12</sup>  $J = 3$  of the former level is observed to be split as shown in Figure 3 whereas  $J = 2$  and 4 appear unperturbed, implying that  $\tilde{a}(1,1,2)^2$  lies slightly lower in energy than calculated relative to  $\tilde{b}(0,1,0)^0$ .

high- $K$  level due to the restricted number of lower state levels populated or in fact known.

The  $\tilde{b}(0,2,0)^0$  level is also expected to be strongly connected to the  $\tilde{a}(0,0,0)$  and  $(0,1,0)$  levels, and some bending hot-band transitions should be observed in the present measurement region. This upper level was actually assigned originally by Herzberg and Johns based on just 3 rotational transitions from the zero-point level of the  $\tilde{a}$  state<sup>5</sup> and not subsequently observed. No lines were observed at the positions estimated based on the previous assignments. Instead, a series of strong transitions that could be assigned to a  $K = 0$  level from the  $\tilde{a}(0,1,0)$  hot vibrational level were observed at other frequencies. We noted that the ratio of the relative intensity of the  $R$ -branch to the  $Q$ -branch transitions to the  $\tilde{b}(0,2,0)^0$  level was larger than for the corresponding transitions to the  $\tilde{b}(0,1,0)^0$  level. In the present data, the  $\tilde{b}(0,2,0)^0$   $7_{07}$  and  $8_{08}$  levels have been assigned. They were identified via transitions from the  $7_{17}$  and  $8_{18}$  levels of  $\tilde{a}(0,1,0)$ . The expected transitions were first calculated by using the molecular constants obtained by Petek et al.<sup>18</sup> for the lower level, together with preliminary fits to the lower- $J$  levels in the upper level measured here. Then, absorption lines with the expected intensity were found within  $1 \text{ cm}^{-1}$  of the predicted frequencies. Term energies of  $7_{17}$  and  $8_{18}$  relative to  $0_{00}$  of  $\tilde{a}(0,1,0)$  are thus determined to be  $444.248$  and  $562.821 \text{ cm}^{-1}$ , respectively, by simply adding the differences to the known energy levels. Along with the increase of  $N$ ,  $K_c$  becomes



**TABLE 3: A Comparison of the Experimentally Determined and Theoretically Predicted Energy Levels**

level	<i>K</i>	experiment	Gu et al. <sup>a</sup>	Green et al. <sup>b</sup>	Duxbury et al. <sup>c</sup>
$\tilde{b}(0,1,0)$	0	9537	9537	9566	9539
$\tilde{b}(0,2,0)$	0	10827	10831	10848	10822
$\tilde{b}(0,0,0)$	4	9711	9754	9716	9621
$\tilde{a}(0,8,0)$	1	9444	9450	-	-

<sup>a</sup> Ref 12. <sup>b</sup> Ref 7. <sup>c</sup> Ref 11.

a good quantum number, and the calculated values of  $7_{07}$  and  $7_{17}$  are 443.6 and 443.8 cm<sup>-1</sup>. A previous dispersed fluorescence study<sup>26</sup> reported a transition involving  $7_{07}$  and derived an energy of 463.01 cm<sup>-1</sup> in the  $\tilde{a}(0,1,0)$  level. However, the  $7_{17}$  level of the present study does not agree with this estimate for the  $7_{07}$  level. Unless there is a very strong perturbation, which is unlikely in  $\tilde{a}(0,1,0)$ , the  $7_{07}$  level previously determined seems rather implausible.

Finally, 21 transitions to another  $K = 1$  level were identified in the data. On the basis of the results of ref 12, we identified this as the  $\tilde{a}(0,8,0)^1$  level, and this is supported by the size of the *l*-type doubling constant, which is determined to be -1.661 cm<sup>-1</sup>. The large negative value is reasonable compared with those of the other bending excited  $\tilde{a}$  states. The calculated doubling constant based on the energy levels by Gu et al.<sup>12</sup> is 1.815 cm<sup>-1</sup>. The absolute value is comparable, even though the sign is opposite, due to a different definition of the rovibronic symmetries, a fact previously noted in  $\tilde{a}(0,9,0)^1$ ,  $\tilde{a}(0,10,0)^1$ , and  $\tilde{a}(0,11,0)^1$ .<sup>32</sup>

A comparison with recent published high-level calculations is given in Table 3. The experimental values of  $K = 0$  levels are in excellent agreement with Gu et al.'s<sup>12</sup> and Duxbury et al.'s<sup>11</sup> results, which is to be expected considering the absence of Renner-Teller coupling in  $K = 0$ . On the other hand, the energy level of the  $\tilde{b}(0,0,0)^4$  level does not agree with the later calculations but does agree rather better with the earlier<sup>7</sup> result. We note that the calculated energy of  $\tilde{a}(3,1,0)^4$  by Gu et al.<sup>12</sup> is 9700 cm<sup>-1</sup>, which is close to the experimental value. However, transitions to this state must have only a weak transition moment. This result clearly suggests the necessity of reevaluating the potential energy surface of the  $\tilde{b}$  state near its equilibrium because modification of the potential needed to improve agreement between observation and calculation at higher energies seems to have resulted in poorer agreement here. Future high-resolution spectroscopy of  $\tilde{b}(0,0,0)^0$ , which lies around 8350 cm<sup>-1</sup>, is needed if the experimental potential energy surface is to be determined more reliably.

Overall, about 80% of observed strong transitions have been assigned, whereas slightly more than 80% of weak transitions remain unassigned. Some of the unassigned lines must involve transitions with high *J* and *K* levels of the  $\tilde{a}(0,0,0)$  and  $\tilde{a}(0,1,0)$  levels whose term values are not known. The possibility for chance coincidences in spectral line frequencies is sufficiently high that most or all of the expected rovibronic transitions to a given upper-state level need to be assigned to be confident of an assignment. In several cases, only one or two possible transitions were identified in the data, in which case the upper level could not be assigned with certainty. Transitions due to <sup>13</sup>C would also be found in the unassigned transitions. Other transitions obeying selection rules of  $\Delta K = \pm 3, 5$  are also candidates for weak transitions; some have been assigned, and others lie outside the scanned region.

The energy separation between  $\tilde{a}(0,0,0)$  and  $\tilde{X}(0,0,0)$  was determined to be  $3147 \pm 5$  cm<sup>-1</sup> following analysis of the LMR<sup>2</sup> spectrum. This separation might be determined precisely through

the observation of the singlet-triplet transitions or  $\tilde{b}-\tilde{X}$  transitions in the visible spectrum. For example, transitions from the  $\tilde{X}(0,0,0)$  level to the  $\tilde{b}(0,0,0)^4$  level detected here would occur in the 12200 cm<sup>-1</sup> region observed previously.<sup>30</sup> However, careful study of the earlier data did not reveal a set of transitions corresponding to  $\Delta J = 0, \pm 1$  within 15 cm<sup>-1</sup> of the estimated  $\Delta E_{ST}$ . The triplet character of these  $\tilde{b}$ -state levels is unknown, and the intensity of such transitions has not been estimated. However, spin-orbit coupling with the  $\tilde{X}$  state is generally smaller in the  $\tilde{b}$  state than in the  $\tilde{a}$  state because the states are only mixed via Renner-Teller mixing of  $\tilde{a}$  state character into the  $\tilde{b}$  level or by some other indirect mechanism. Energy levels of  $\tilde{X}^3B_1$  are not known in this high-energy region. Since it is already known<sup>1,18</sup> that some levels in  $\tilde{X}(0,2,0)$ ,  $\tilde{X}(0,3,0)$ , and  $\tilde{a}(0,0,0)$  have mixed singlet and triplet character, it seems plausible that one might observe direct absorption involving these levels. In fact, several transitions involving such levels are observed in the present measurement. Observation of infrared vibration-rotation transitions from  $\tilde{X}(0,0,0)$  or  $\tilde{X}(0,1,0)$  to  $\tilde{X}(0,2,0)$ ,  $\tilde{X}(0,3,0)$ , and  $\tilde{a}(0,0,0)$  might therefore be used to determine the absolute singlet-triplet separation. Published calculated intensities of vibrational transitions in  $\tilde{X}^3B_1$  and  $\tilde{a}^1A_1$  vary between the various studies.<sup>36-39</sup> However, given a nonzero vibrational transition moment in the triplet state, there is a good possibility for their observation. We plan an attempt to observe infrared transitions between these levels and hope to determine the singlet-triplet separation accurately. An accurate knowledge of the separation would also help to assign weak triplet-singlet transitions that no doubt lie among the unassigned lines in the near-infrared and visible spectrum.

## Summary

Methylene is a prototype for all bivalent carbon species, and these absorption spectra in the near-infrared region provide new information on four vibronic levels that lie between 9400 and 10 800 cm<sup>-1</sup> above the zero-point level of the  $\tilde{a}$  state of the molecule. Three of these levels had not previously been observed, whereas rotational levels of the last, originally reported over 30 years ago, are found to be 4 cm<sup>-1</sup> higher than the original assignment. The levels include the lowest so far detected in the  $\tilde{b}^1B_1$  state of CH<sub>2</sub> and provide information on a region of the molecule's potential energy surface that has not previously been available. The results will be of use in future refinements of the singlet potential energy surfaces of CH<sub>2</sub> and in particular suggest some adjustment of the  $\tilde{b}$  state PES near its minimum. Analysis also provided estimated energies for two,  $7_{17}$  and  $8_{18}$ , rotational levels in the  $\tilde{a}(0,1,0)$  level that had not previously been identified, adding to the knowledge base of singlet CH<sub>2</sub> rotational energies that are accurately known. Near-infrared diode laser absorption spectroscopy is a relatively new high-resolution tool that is straightforward to apply and will find uses in future kinetic and dynamical studies of this and other radicals with low-lying excited electronic states.

**Acknowledgment.** The authors thank Professor Per Jensen for providing details of his calculations of CH<sub>2</sub> energy levels prior to publication. Work at Brookhaven National Laboratory was carried out under Contract No. DE-AC02-98CH10886 with the U.S. Department of Energy and is supported by its Division of Chemical Sciences, Office of Basic Energy Sciences.

## References and Notes

- (1) McKellar, A. R. W.; Bunker, P. R.; Sears, T. J.; Evenson, K. M.; Saykally, R. J.; Langhoff, S. R. *J. Chem. Phys.* **1983**, *79*, 5251.

- (2) Jensen, P.; Bunker, P. R. *J. Chem. Phys.* **1988**, *89*, 1327.
- (3) Herzberg, G. *Molecular Spectra and Molecular Structure III: Electronic Spectra and Electronic Structure of Polyatomic Molecules*; Van Nostrand-Reinhold: New York, 1966.
- (4) Herzberg, G. *Proc. R. Soc. London, Ser. A* **1961**, *262*, 291.
- (5) Herzberg, G.; Johns, J. W. C. *Proc. R. Soc. London, Ser. A* **1966**, *295*, 107.
- (6) Johns, J. W. C.; Ramsay, D. A.; Ross, S. C. *Can. J. Phys.* **1976**, *54*, 1804.
- (7) Green, W. H., Jr.; Handy, N. C.; Knowles, P. J.; Carter, S. *J. Chem. Phys.* **1991**, *94*, 118.
- (8) Duxbury, G.; Jungen, C. *Mol. Phys.* **1988**, *63*, 981.
- (9) Alijah, A.; Duxbury, G. *Mol. Phys.* **1990**, *70*, 981.
- (10) Duxbury, G.; McDonald, B. D.; Van Gogh, M.; Alijah, A.; Jungen, C.; Palivan, H. *J. Chem. Phys.* **1998**, *108*, 2336.
- (11) Duxbury, G.; Alijah, A.; McDonald, B. D.; Jungen, C. *J. Chem. Phys.* **1998**, *108*, 2351.
- (12) Gu, J.-P.; Hirsch, G.; Buenker, R. J.; Brumm, M.; Osmann, G.; Bunker, P. R.; Jensen, P. *J. Mol. Struct.* **2000**, *247*, 517–8.
- (13) Jensen, P.; Brumm, M.; Kraemer, W. P.; Bunker, P. R. *J. Mol. Spectrosc.* **1995**, *171*, 31.
- (14) Kolbuszewski, M.; Bunker, P. R.; Kraemer, W. P.; Osmann, G.; Jensen, P. *Mol. Phys.* **1966**, *88*, 105.
- (15) Lengel, R. K.; Zare, R. N. *J. Am. Chem. Soc.* **1978**, *100*, 7495.
- (16) Feldmann, D.; Meier, K.; Zacharias, H.; Welge, K. H. *Chem. Phys. Lett.* **1978**, *59*, 171.
- (17) Petek, H.; Nesbitt, D. J.; Darwin, D. C.; Moore, C. B. *J. Chem. Phys.* **1987**, *86*, 1172.
- (18) Petek, H.; Nesbitt, D. J.; Moore, C. B.; Birss, F. W.; Ramsay, D. A. *J. Chem. Phys.* **1987**, *86*, 1189.
- (19) Petek, H.; Nesbitt, D. J.; Ogilby, P. R.; Moore, C. B. *J. Phys. Chem.* **1983**, *87*, 5367.
- (20) Petek, H.; Nesbitt, D. J.; Darwin, D. C.; Ogilby, P. R.; Moore, C. B.; Ramsay, D. A. *J. Chem. Phys.* **1987**, *91*, 6566.
- (21) Feldmann, D.; Meier, K.; Schmiedl, R.; Welge, K. H. *Chem. Phys. Lett.* **1978**, *60*, 30.
- (22) Xie, W.; Harkin, C.; Dai, H. L.; Green, W. H., Jr.; Zheng, Q. K.; Mahoney, A. J. *J. Mol. Spectrosc.* **1989**, *138*, 596.
- (23) Xie, W.; Harkin, C.; Dai, H.-L. *J. Chem. Phys.* **1990**, *93*, 4615.
- (24) Hartland, G. V.; Dai, H.-L. Dispersed and Stimulated Emission Studies of the Excited Vibrational Levels of a Transient Molecule: Singlet Methylene. In *Molecular Dynamics and Spectroscopy by Stimulated Emission Pumping*; Dai, H.-L., Field, R. W., Eds.; World Scientific: Singapore, 1995.
- (25) Hartland, G. V.; Qin, D.; Dai, H.-L. *J. Chem. Phys.* **1993**, *98*, 2469.
- (26) Garcia-Moreno, I.; Moore, C. B. *J. Chem. Phys.* **1993**, *99*, 6429.
- (27) Hartland, G. V.; Qin, D.; Dai, H.-L. *J. Chem. Phys.* **1995**, *102*, 6641.
- (28) Green, W. H., Jr.; Chen, I.-C.; Bitto, H.; Guyer, D. R.; Moore, C. B. *J. Mol. Spectrosc.* **1989**, *138*, 614.
- (29) Qin, D.; Hartland, G. V.; Dai, H.-L. *J. Mol. Spectrosc.* **1994**, *168*, 333.
- (30) Chang, B.-C.; Wu, M.; Hall, G. E.; Sears, T. J. *J. Chem. Phys.* **1994**, *101*, 9236.
- (31) Fockenber, C.; Marr, A. J.; Sears, T. J.; Chang, B.-C. *J. Mol. Spectrosc.* **1998**, *187*, 119.
- (32) Marr, A. J.; Sears, T. J.; Chang, B.-C. *J. Chem. Phys.* **1998**, *109*, 3431.
- (33) Hall, G. E.; North, S. W. Transient Laser Frequency Modulation Spectroscopy. In *Annual Review of Physical Chemistry*; Strauss, H. L., Babcock, G. J., Leone, S. R., Eds.; Annual Reviews, Inc.: Palo Alto, CA, 2000; Vol. 51.
- (34) Trutna, W. R.; Byer, R. L. *Appl. Opt.* **1980**, *19*, 301.
- (35) Pilgrim, J. S.; Jennings, R. T.; Taatjes, C. A., *Rev. Sci. Instrum.* **1997**, *68*, 1875.
- (36) Bunker, P. R.; Langhoff, S. R. *J. Mol. Spectrosc.* **1983**, *102*, 204.
- (37) Jensen, P. *J. Mol. Spectrosc.* **1988**, *132*, 429.
- (38) Yamaguchi, Y.; Schaefer, H. F., III. *Chem. Phys.* **1997**, *225*, 23.
- (39) Das, D.; Whittenburg, S. L. *J. Mol. Struct.* **1999**, *492*, 175.